Available online at www.sciencedirect.com

ScienceDirect

Procedia CIRP 62 (2017) 62 – 67

www.elsevier.com/locate/procedia

10th CIRP Conference on Intelligent Computation in Manufacturing Engineering - CIRP ICME '16

Influence of curved workpiece contours on delamination during end milling of FRP

Wolfgang Hintze*, Felix Brügmann

Hamburg University of Technology, Institute of Production Management and Technology, Denickestraße 17, 21071 Hamburg, Germany

* Corresponding author. Tel.: +49-40-42878-3051; fax: +49-40-42878-2295. *E-mail address:* w.hintze@tuhh.de

Abstract

When end milling long fiber reinforced composites, fiber protrusions of the top layers can occur. The lengths of fiber protrusions found on real workpieces with curved contours cannot be explained so far.
The lengths of individual fibers to be cut along the tool path depend on tool diameter, local fiber orientation and path geometry. All fibers are separated into two ends at the initial contact with the tool. They define the theoretical maximum lengths of fiber protrusions.
A model for these observations has been established. The model is validated by milling experiments using curved contours.
© 2017 The Authors. Published by Elsevier B.V. This is an open access article under the CC BY-NC-ND license (http://creativecommons.org/licenses/by-nc-nd/4.0/).
Peer-review under responsibility of the scientific committee of the 10th CIRP Conference on Intelligent Computation in Manufacturing Engineering

Keywords: Modelling; Composite; Milling

1. Introduction

Fiber reinforced plastics (FRP) are established lightweight materials which are increasingly used in recent years especially in the aircraft industry. Although FRP parts are produced near net shape, they need edge trimming which is often done by end milling [1, 2].

When milling FRP, the top layers of the laminate can be damaged by chipping and protruding fibers. Such delamination of crimped and non-crimped fabrics is a serious problem [3] and has been described in several publications [4, 5, 6, 7, 8, 9, 10].

In order to avoid delamination, tool concepts and cutting edge geometries [11, 12, 13], wear-resistant cutting materials [14, 15, 16], the influence of cutting parameters [6, 17] and special machining strategies [4, 18, 19] have been proposed and analyzed. Nevertheless, delamination still occurs and makes reworking necessary, leading to higher production costs and times and sometimes resulting in irreparable loss of the parts.

Previous investigations on delamination phenomena of non-crimped fabrics (NCF) [4, 6, 17, 20, 21] as well as crimped fabrics [10] have been conducted using milling processes with linear feed direction. When milling FRP parts made of NCF with unidirectional top layers, it was observed that the type of delamination and especially the length of fiber protrusions vary at different positions along the workpiece contour. As real-life workpieces show convex and concave areas along their contour, consideration of non-linear feed directions seems necessary for an in-depth understanding of delamination phenomena. Therefore, the length of fiber protrusions depending on feed direction is the subject of the following study.

2. Theoretical consideration of delamination and fiber protrusion when milling FRP

Colligan and Ramulu [6] introduced three different types of delamination. Type 1 describes a surface break-out of fiber bundles within the uncut top layers starting at the trimmed edge. Type 2 delamination refers to fibers protruding into the milling path without any other damage to the workpiece. A common form of delamination is a combination of type 1 and 2, since each fiber protrusion inevitably leads to at least minimal damage at the trimmed edge [10, 22]. Type 3 delamination describes loose fiber ends.

2212-8271 © 2017 The Authors. Published by Elsevier B.V. This is an open access article under the CC BY-NC-ND license (http://creativecommons.org/licenses/by-nc-nd/4.0/).
Peer-review under responsibility of the scientific committee of the 10th CIRP Conference on Intelligent Computation in Manufacturing Engineering
doi:10.1016/j.procir.2016.06.115

The fiber position relative to the feed direction v_f is defined by the fiber orientation angle ϕ, which is measured counterclockwise between v_f and the fiber axis direction. Puw and Hocheng [23] showed that the fiber orientation angle ϕ has a significant influence on the type and appearance of delamination. Due to the rotation of the tool, the fiber cutting angle θ, defined between cutting direction v_c and the axis of the uncut fiber, varies continuously.

When milling, the lengths of individual fibers to be cut along the tool path depend on tool diameter, local fiber orientation and path geometry. According to Hintze [5], delamination starts at the initial contact between tool and fiber, which simultaneously represents the initial separation point of the fiber. The fiber cutting angle at the separation point is always $\theta_{initial} = 180°$. After initial separation and no further cutting of the fiber afterwards, two loose ends of fibers protrude into the milling path. Their length is significantly influenced by the fiber orientation ϕ [5].

The following calculation of the maximum theoretical lengths of fiber protrusions is carried out for a tool rotating clockwise with a feed direction parallel to the laminate plane. It is assumed that every cutting edge initially separates just one single fiber per revolution.

2.1. Lengths of fiber protrusions for linear feed direction

When milling along a linear feed path, the position of the initial fiber separation point only depends on the tool diameter d_{tool} and the current fiber orientation $\phi_{initial}$, see Fig. 1. In this case, the fiber orientation angle at initial contact $\phi_{initial}$ is the same as the fiber cutting angle at the trimmed edge θ_{edge}.

The length of an individual fiber crossing a linear feed path, l_{lin}, is given by:

$$l_{lin} = \frac{d_{tool}}{\sin(\phi_{initial})} \tag{1}$$

The distance of the initial separation point $x_{initial}$ of the fiber measured perpendicular to the up-milling edge is:

$$x_{initial} = \frac{d_{tool}}{2} \cdot \left(1 + \cos\left(\phi_{initial}\right)\right) \tag{2}$$

The maximum lengths of the fiber protrusion ending at the down-milling edge $l_{lin,down}$ and of the fiber protrusion ending at the up-milling edge $l_{lin,up}$ are:

$$l_{lin,down} = \frac{d_{tool} \cdot \left(1 - \cos\left(\phi_{initial}\right)\right)}{2 \cdot \sin\left(\phi_{initial}\right)} \tag{3}$$

$$l_{lin,up} = \frac{d_{tool} \cdot \left(1 + \cos\left(\phi_{initial}\right)\right)}{2 \cdot \sin\left(\phi_{initial}\right)} \tag{4}$$

Fig. 2 shows the maximum lengths of fiber protrusions ending at the up- and down-milling edge depending on the initial fiber orientation angle $\phi_{initial}$ for two tool diameters $d_{tool} = 4$ mm and $d_{tool} = 12.7$ mm using equations (3) and (4). Apparently, the fiber protrusions on both sides are symmetrical to the fiber orientation angle $\phi_{initial} = 90°$. The possible lengths of fiber protrusions for the down-milling edge increase with $\phi_{initial}$, whereas for the up-milling edge they decrease with $\phi_{initial}$. At $\phi_{initial} = 90°$, the length of fiber protrusions at both edges are identical.

The lengths of fiber protrusions approach infinity for $\phi_{initial} \rightarrow 0°$ and for $\phi_{initial} \rightarrow 180°$. Obviously, the work piece dimensions always limit the length of fiber protrusions. For $\phi_{initial} = 0°/180°$, though, no fiber protrusion can occur due to the parallel orientation of fiber axis and feed direction.

In addition to the fiber orientation angle, the tool diameter correlates with the possible lengths of fiber protrusions, see Fig. 2. Compared to fiber orientation angle and milling direction (up / down), the tool diameter has a minor influence on the lengths of fiber protrusions.

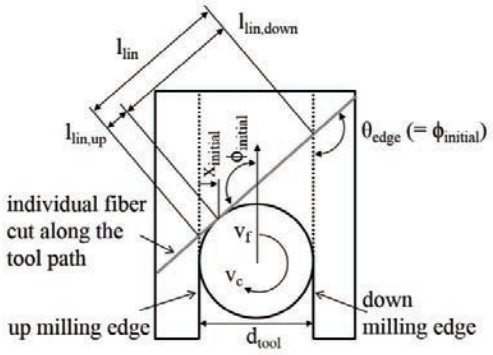

Fig. 1. Initial fiber contact in milling along a linear feed path

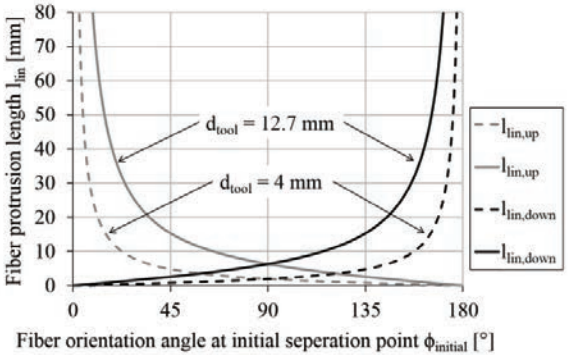

Fig. 2. Fiber protrusion lengths dependent on $\phi_{initial}$ and d_{tool}

2.2. Lengths of fiber protrusions for non-linear feed direction

In order to investigate the formation of fiber protrusions when milling real parts with curved contours, the maximum theoretical lengths of fiber protrusions are now modeled for a circular feed path, see Fig. 3.

In contrast to a linear feed direction, the fiber orientation angle ϕ varies continuously along a circular milling path which leads to $\phi_{initial}$ being unequal to θ_{edge} of the considered fiber. This effect is shown in Fig. 3 for two fibers cut under $\phi_{initial} = 90°$ at different feed directions whose fiber cutting angles at the outer edge are $\theta_{edge} > 90°$ for clockwise feed direction and $\theta_{edge} < 90°$ for counterclockwise feed direction, respectively.

The cutting direction v_c at the trimmed edge is always tangential to the workpiece contour. Therefore, the feed direction v_f and the tool diameter d_{tool} have no influence on the fiber cutting angle at the edge when the fiber orientation remains constant relative to the workpiece.

In case of a non-linear feed path after initial separation of a fiber under a certain fiber orientation angle $\phi_{initial}$, the maximum length of fiber protrusions differ compared to a linear feed path. The difference Δl_{circle} is shown in Fig. 4 for the down-milling side of a circle with counterclockwise feed direction.

The fiber lengths for the linear feed direction corresponding to the down- and up-milling edge are denoted by $l_{lin,down}$ and $l_{lin,up}$ while for the circular feed direction they are referred to as $l_{circ,down}$ and $l_{circ,up}$. For simplicity of subsequent calculations, the two mentioned fiber lengths for linear feed direction are named l_{linear} and the two mentioned fiber lengths for circular feed direction are named l_{circle}.

As shown in Fig. 3, there are three distinct areas that need to be handled separately. In area I, the two ends of the separated fibers end on the inner and outer edge of the circular tool path, R_{inner} and R_{outer} respectively. In area II and III, both ends of separated fibers end on the outer edge. Area II and III are symmetrically distributed to the fiber orientation angle of $\phi_{initial} = 0°/180°$ with an angle-range of two times $\Delta\theta_{edge}$.

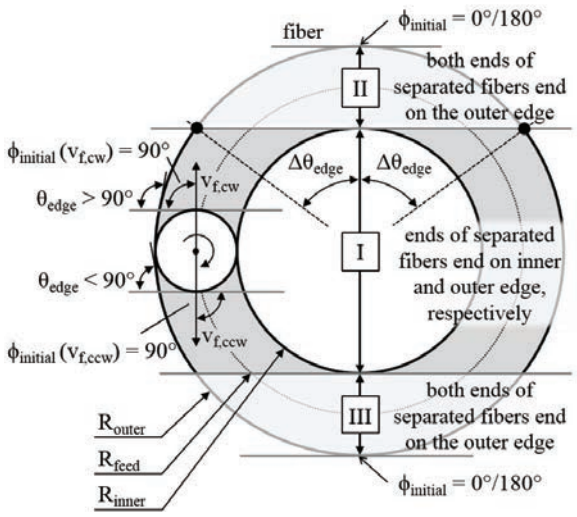

Fig. 3. Three different areas of fiber protrusions at circular feed direction

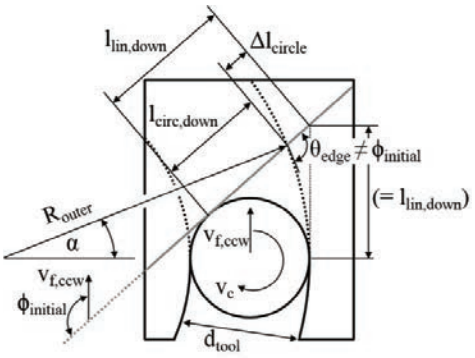

Fig. 4. Length of a fiber in the milling path for non-linear feed direction

The half angle-range $\Delta\theta_{edge}$ follows from calculating the secant to the outer circle which is a tangent to the inner circle at the same time, see Fig. 3.

$$\Delta\theta_{edge} = \arccos\left(\frac{R_{outer} - d_{tool}}{R_{outer}}\right) \tag{5}$$

Regarding area I, the maximum fiber protrusion length in case of a circular feed path can be defined by the following calculations. The inner and outer radius R_{inner} and R_{outer} of the circular tool path are named R in these equations:

$$l_{circle} = l_{linear} \pm \Delta l_{circle} \tag{6}$$

$$\left(l_{linear} + \Delta l_{circle}\cos\left(\phi_{initial}\right)\right)^2 + \left(R - \Delta l_{circle}\sin\left(\phi_{initial}\right)\right)^2 = R^2 \tag{7}$$

Solution of the quadratic equation (7) leads to:

$$\Delta l_{circle} = -\left(l_{linear}\cdot\cos\left(\phi_{initial}\right) - R\cdot\sin\left(\phi_{initial}\right)\right) - \sqrt{\left(l_{linear}\cdot\cos\left(\phi_{initial}\right) - R\cdot\sin\left(\phi_{initial}\right)\right)^2 - l_{linear}^2} \tag{8}$$

Depending on whether milling is carried out in clockwise direction $v_{f,cw}$ or in counterclockwise direction $v_{f,ccw}$ the following values of Δl_{circle} in equation (6), l_{linear} and R have to be used in equation (8):

- for $l_{circ,down}$ ($v_{f,cw}$) + Δl_{circle}; $l_{linear} = l_{lin,down}$; $R = R_{inner}$
- for $l_{circ,up}$ ($v_{f,cw}$) - Δl_{circle}; $l_{linear} = l_{lin,up}$; $R = R_{outer}$
- for $l_{circ,down}$ ($v_{f,ccw}$) - Δl_{circle}; $l_{linear} = l_{lin,down}$; $R = R_{outer}$
- for $l_{circ,up}$ ($v_{f,ccw}$) + Δl_{circle}; $l_{linear} = l_{lin,up}$; $R = R_{inner}$

The angle α (Fig. 4) represents the difference between the fiber orientation angle $\phi_{initial}$ at the initial contact point and the fiber cutting angle θ_{edge} at the trimmed edge of a certain fiber. It can be calculated by the following equation:

$$\alpha = \arccos\left(\frac{R - \Delta l_{circle}\cdot\sin\left(\phi_{initial}\right)}{R}\right) \tag{9}$$

For calculation of α in case an edge is machined by down-milling in clockwise feed direction, $R = R_{inner}$ is used in equation (9), for the up-milling edge $R = R_{outer}$ is used accordingly. For counterclockwise feed direction, R_{inner} and R_{outer} switch positions. The fiber cutting angle at the trimmed edge θ_{edge} is calculated for clockwise feed direction by adding α to $\phi_{initial}$ and for counterclockwise feed direction by subtracting α from $\phi_{initial}$.

$$\theta_{edge,cw} = \phi_{initial} + \alpha; \quad \theta_{edge,ccw} = \phi_{initial} - \alpha \tag{10, 11}$$

For areas II and III, where both fiber ends meet the outer concave edge of the circular slot, the maximum fiber protrusion length $l_{circle,2,3}$ is given by (with l_{circle} from eq. (6)):

$$l_{circle,2,3} = 2 \cdot \sin(\phi_{initial}) \cdot R_{outer} - l_{circle} \tag{12}$$

The corresponding fiber cutting angle at the edge $\theta_{edge,2,3}$ of the second end of the fiber that cannot be calculated with the formulas for area I is given by (with θ_{edge} from eq. (10, 11)):

$$\theta_{edge,2,3} = 180° - \theta_{edge} \tag{13}$$

Both the maximum fiber protrusion lengths and the related fiber cutting angles at the trimmed edge θ_{edge} calculated with the previously presented equations allow prediction of the maximum length of fiber protrusions for a circular tool path. The maximum fiber protrusion lengths are point symmetric to the circle center point. Hence, the examination of maximum fiber protrusions in a half circle is sufficient. Fig. 5 shows the maximum fiber protrusions for the inner and outer edge of the left half of a circular path for counterclockwise feed direction.

On the outer edge, a sudden increase of the maximum fiber protrusion length can be observed in the transition region at around $\phi_{initial}$ = 0°/180°, see Fig. 5 a). This represents the transition between area I and II or area I and III respectively. The longest possible fiber protrusion at the outer edge arises at the tangent to the inner edge, where delamination is not stopped by the inner edge.

On the inner edge, see Fig. 5 b), a sudden drop can be observed at an initial fiber orientation angle of $\phi_{initial}$ = 0°/180°, which coincides with the transition from longest to smallest possible fiber protrusion length.

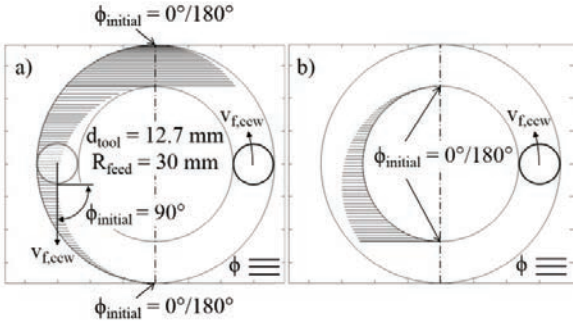

Fig. 5. Fiber protrusions on left half circle: a) outer edge; b) inner edge

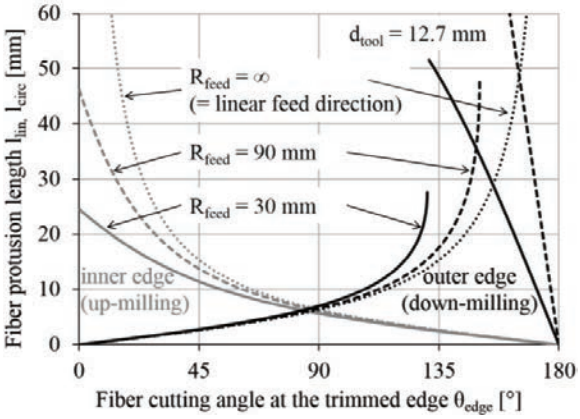

Fig. 6. Calculated fiber protrusion lengths (counterclockwise feed direction)

Besides the parameters influencing the maximum fiber protrusion length at linear feed direction (derived in section 2.1) such as tool diameter, feed direction and fiber orientation angle, the radius of the circular tool path is an important influencing parameter regarding non-linear feed directions, see Fig. 6.

With increasing radius of the circle and with decreasing fiber cutting angles at the trimmed edge θ_{edge}, the maximum fiber protrusion length increases progressively for the inner edge at counterclockwise feed direction, see Fig. 6. For the outer edge, the fiber protrusion lengths reach their maximum at the transition between area I and II or area I and III at a specific θ_{edge}. In case of counterclockwise feed direction, θ_{edge} is given by $\theta_{edge} = 180° - \Delta\theta_{edge}$ and in case of clockwise feed direction by $\theta_{edge} = 0° + \Delta\theta_{edge}$.

3. Experimental investigation of fiber protrusions

In order to verify the model developed in section 2, milling tests with circular feed paths were conducted on parts made of carbon fiber reinforced plastics (CFRP). Half circles of radii $R_{feed,1}$ = 30 mm, $R_{feed,2}$ = 60 mm and $R_{feed,3}$ = 90 mm were machined using clockwise and counterclockwise feed direction.

The cutting velocity was v_c = 511 m/min and the feed per tooth f_z = 0.03 mm. In order to investigate the sudden increase of the fiber protrusion lengths at $\phi_{initial}$ = 0°/180° as predicted by the model, a fiber cutting angle of θ_{edge} = 90° was selected at the beginning and at the end of the half circles.

The CFRP used in the tests was NCF consisting of M21E resin and IMA-fibers with a laminate structure of 0°/90° and an overall thickness of t = 6 mm. The top layer was made of unidirectional CFRP while the bottom layer was made of copper mesh.

The tests were carried out using a milling machine made by Reichenbacher (Vision II) with a spindle power of 24 kW and a maximum speed of 24.000 rpm. The workpieces were fixed by clamping claws around the milling contour. The unidirectional top layer was on the upper side. The used tool with a diameter of d_{tool} = 12.7 mm was a common double-edged PCD end mill with a twist angle of γ_p = 0°, a rake angle of γ_f = 0°and a clearance angle of α_f = 12°.

In order to obtain fiber protrusions at the machined edges, a tool of defined wear state (cutting edge radius $r_n \approx 34$ µm before and after the tests) was used. A low cutting speed, as used in these experiments, stimulates the formation of fiber protrusions as well.

The fiber protrusions were analyzed and documented using a microscope made by Olympus (type SZX10) which was connected to a digital camera to evaluate the lengths at the computer. The fiber protrusion lengths were measured in longitudinal direction of the fibers in steps of 5° at the trimmed edge.

4. Results and discussion

Fig. 7 shows the fiber protrusions at different radii and feed directions of the milled half circles. It can be seen that fiber protrusions (type 2 delamination) occur on every inner and outer edge with varying lengths.

In all tests, the longest fiber protrusions were found on the outer edge. Areas with very small fiber protrusions can be identified on the inner and outer edges. For the half circles milled in clockwise feed direction, the smallest fiber protrusions occurred on the inner edge between $135° < \theta_{edge} < 180°$ and for the outer edge between $0° < \theta_{edge} < 45°$ and vice versa for counterclockwise feed direction.

Fig. 8 contains measurement data of fiber protrusion lengths of the parts shown in Fig. 7 for radii $R_{feed,1} = 30$ mm and $R_{feed,3} = 90$ mm milled in clockwise and counterclockwise direction. For comparison with the model, the calculated maximum fiber protrusion lengths are indicated as well.

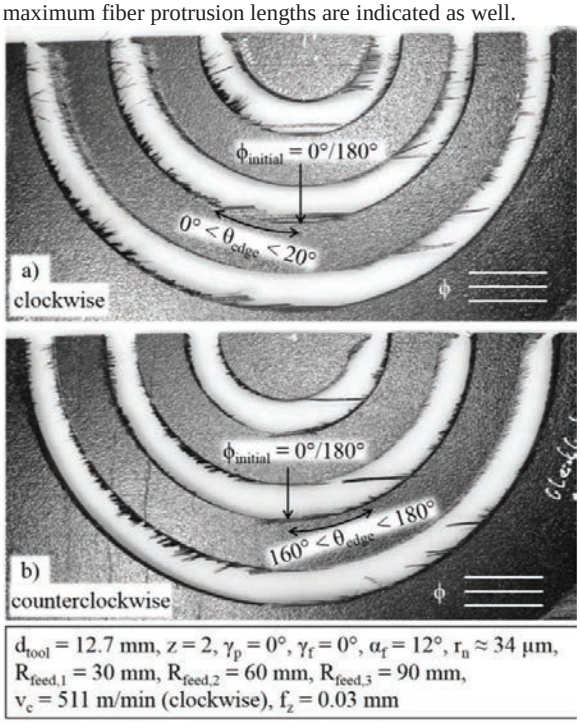

Fig. 7. Fiber protrusions on milled circles: a) clockwise; b) counterclockwise

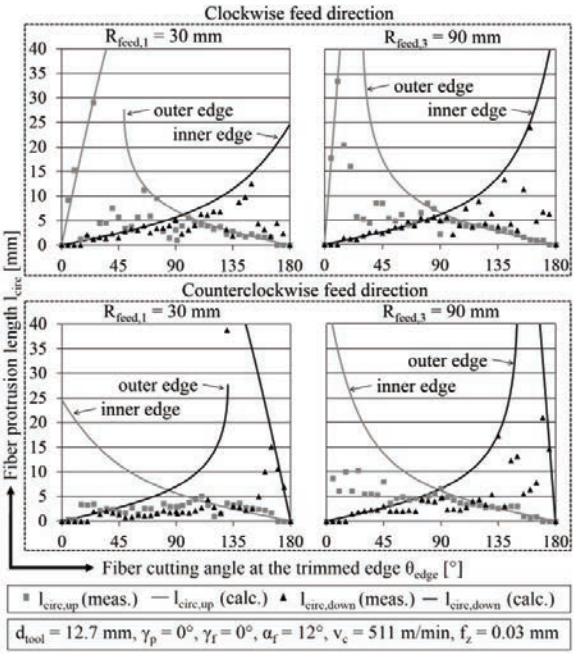

Fig. 8. Measured and calculated fiber protrusion lengths

The range of fiber cutting angles with the smallest calculated maximum fiber protrusion lengths correlate with the smallest measured values. This also applies for the highest calculated and measured lengths of fiber protrusions.

All measured fiber protrusion lengths are very close to the calculated values or below. Very few outliers differ in positive direction and are caused by measurement inaccuracies of partly strongly frayed and kinked fiber protrusions.

When milling in clockwise direction, the outer edge is machined by up-milling and in counterclockwise direction by down-milling. In both situations, the calculation of fiber protrusion lengths shows a sudden increase of the protrusion length that is not found explicitly in the measured values. It can be seen that the maximum measured fiber protrusion length is found closer to the fiber cutting angle of $\theta_{edge} = 0°/180°$ when the circle radius increases. This correlation is also evident in equation (5), as the area where both fiber ends meet the outer edge is symmetrically distributed around $\phi_{initial} = 0°/180°$ with $\Delta\theta_{edge}$ and decreases with higher circle radii.

At linear feed direction, see Fig. 2, the maximum lengths of fiber protrusions from the up- and down-milling edges are symmetrical to the fiber cutting angle $\theta_{edge} = 90°$ ($= \phi_{initial}$). Regarding non-linear feed directions, the distribution is unsymmetrical, which is demonstrated by the calculated and measured values of fiber protrusion lengths, Fig. 7 and Fig. 8.

For all used circle radii, the calculated and measured fiber protrusion lengths correspond up to a length of approximately $l_{circ} = 5$ mm, only. For higher calculated lengths, the majority of the measured values is significantly smaller than predicted by the model. A clear correlation for longer fiber protrusions is found on the outer edge machined in clockwise direction between $0° < \theta_{edge} < 20°$ and for the counterclockwise feed

direction between $160° < \theta_{edge} < 180°$. This observation can also be seen in Fig. 7, where the fiber protrusions almost form a secant to the outer edge in this angle range. Here, fiber protrusion lengths measured after the tests were mostly shorter than the calculated maximum. The explanation for this behavior is undefined breaking of long fiber protrusions due to impacts caused by several consecutive tool contacts, which increase with growing maximum fiber protrusion length.

5. Conclusion and outlook

Delamination avoidance in manufacturing of FRP components is still a challenge with regard to production time and costs. The presented analytical and experimental study reveals the workpiece geometry in combination with tool diameter and feed direction to be important parameters on the occurrence of fiber protrusions.

An analytical model of maximum fiber protrusion lengths of curved contours was derived and the following conclusions have been drawn:

- The fiber protrusion length gets smaller the closer the initial fiber separation point is to the trimmed edge.
- The maximum possible length of fiber protrusions of a single fiber is related to the fiber orientation at the initial fiber separation point $\phi_{initial}$ and is influenced by a non-linear feed direction after initial separation.
- Considering a given milling contour and fiber orientation, the maximum possible fiber protrusion lengths on up- and down-milling edges only depend on feed direction and tool diameter, while the latter shows a positive correlation with the maximum fiber protrusion lengths.
- When milling circular contours, the maximum possible fiber protrusion length is on the outer edge and all protrusions decrease with smaller circle radii.

Experiments verify the calculated maximum fiber protrusion lengths for circular feed paths of various radii. The developed model is applicable to any long fiber reinforced composite with unidirectional top layers. The findings contribute to optimized milling strategies avoiding delamination in FRP machining. Further research should focus on mechanisms of separation or delamination propagation of both fiber ends after initial fiber separation.

References

[1] Ehrenstein GW. Faserverbund-Kunststoffe. Werkstoffe, Verarbeitung, Eigenschaften. München: Hanser; 2006.

[2] Sheikh-Ahmad JY. Machining of polymer composites. New York, London: Springer; 2009.

[3] Gordon S, Hillery MT. A review of the cutting of composite materials. In: Proceedings of the Institution of Mechanical Engineers, Part L: Journal of Materials Design and Applications 2003; 217 (1). p. 35–45.

[4] Hartmann D. Delamination an Bauteilkanten beim Umrissfräsen kohlenstofffaserverstärkter Kunststoffe. Dissertation. Techn. Univ. Hamburg-Harburg, Inst. für Produktionsmanagement u.-technik; 2012.

[5] Hintze W, Hartmann D, Schütte C. Occurrence and propagation of delamination during the machining of carbon fibre reinforced plastics (CFRPs) – An experimental study. In: Composites Science and Technology 2012; 71 (15). p. 1719–1726.

[6] Colligan K, Ramulu M. Delamination in surface plies of graphite/epoxy caused by the edge trimming process. In: Processing and Manufacturing of Composite Materials 1991; Vol. 27.

[7] Jain S, Yang DCH. Delamination-Free Drilling of Composite Laminates. In: J. Eng. for Industry 1994; 116 (4). p. 475–481.

[8] Iliescu D. Experimental and numerical approaches of machining of dry carbon/epoxy composites. Arts et Métiers ParisTech; 2008.

[9] Henerichs M, Voß R, Kuster F, Wegener K. Machining of carbon fiber reinforced plastics. Influence of tool geometry and fiber orientation on the machining forces. In: CIRP Journal of Manufacturing Science and Technology 2015; 9. p. 136–145.

[10] Hintze W, Cordes M, Koerkel G. Influence of weave structure on delamination when milling CFRP. In: Journal of Materials Processing Technology 2015; 216. p. 199–205.

[11] Klocke F, Würtz C, Rummenhöller S. Werkzeugauslegung für die Fräsbearbeitung kohlenstoffaserverstärkter Kunststoffe. In: VDI-Z AOU 1996; p. 52–54.

[12] Masek P, Zeman P, Kolar P. Development of a cutting tool for composites with thermoplastic matrix. In: Maschinenmarkt 2013; p. 422-426.

[13] Teti R. Machining of Composite Materials. In: CIRP Annals - Manufacturing Technology 2002; 51 (2). p. 611–634.

[14] Hohensee V. Umrissbearbeitung faserverstärkter Kunststoffe durch Fräsen und Laserschneiden: VDI Verlag (Fortschritt-Berichte VDI.: Fertigungstechnik); 1992.

[15] Hocheng H, Puw HY. Milling of continuous carbon fiber-reinforced epoxy. In: Processing and Manufacturing of Composite Materials 1991; Bd. 1, p. 65–76.

[16] Klocke F, Koenig W, Rummenhoeller S, Wuertz C. Milling of advanced composites. In: Manufacturing Engineering and Materials Processing 1999; 53. p. 249–266.

[17] Davim JP, Reis P. Damage and dimensional precision on milling carbon fiber-reinforced plastics using design experiments. In: Journal of Materials Processing Technology 2005; 160 (2). p. 160–167.

[18] Becke C. Prozesskraftrichtungsangepasste Fräs„strategien zur schädigungsarmen Bohrungsbearbeitung an faserverstärkten Kunststoffen. Dissertation. Universität Karlsruhe, Karlsruher Institut für Technologie (KIT); 2011.

[19] Geis T, Klingelhöller C, Hintze W. Constant Depth Scoring of Fibre Reinforced Plastic Structures to Prevent Delamination. In: Procedia CIRP 2014; 14, p. 205–210.

[20] Colligan K, Ramulu M. The effect of edge trimming on composite surface plies. In: Manufacturing Review (USA) 1992; 5 (4), p. 274–283.

[21] Hocheng H, Puw HY, Huang Y. Preliminary study on milling of unidirectional carbon fibre-reinforced plastics. In: Composites Manufacturing 1993; 4 (2), p. 103–108.

[22] Hintze W, Hartmann D. Modeling of Delamination During Milling of Unidirectional CFRP. In: Procedia CIRP 2013; 8, p. 444–449.

[23] Puw HY, Hocheng H. Machinability test of carbon fiber-reinforced plastics in milling. In: Materials and Manufacturing Processes 1993; 8 (6), p. 717–729.